Acta Diabetologica (2019) 56:1013–1022
https://doi.org/10.1007/s00592-019-01335-4

ORIGINAL ARTICLE

Glucose metabolism during tumorigenesis in the genetic mouse model of pancreatic cancer

Valentina Pasquale[1] · Erica Dugnani[1] · Daniela Liberati[2] · Paolo Marra[3] · Antonio Citro[1] · Tamara Canu[3] · Martina Policardi[1] · Libera Valla[1] · Antonio Esposito[3,4] · Lorenzo Piemonti[1,4]

Received: 4 March 2019 / Accepted: 28 March 2019 / Published online: 15 April 2019

Abstract

Aim More than 40% of pancreatic ductal adenocarcinoma (PDAC) patients have glucose intolerance or diabetes. The association has led to two hypotheses: PDAC causes diabetes or diabetes shares risk factors for the development of PDAC. In order to elucidate the relationship between diabetes and PDAC, we investigated the glucose metabolism during tumorigenesis in the *LSL-Kras*$^{G12D/+}$*; LSL-Trp53*$^{R172H/+}$; and *Pdx-1-Cre* (KPC) mouse, a genetically engineered model of PDAC.

Methods Male and female KPCs have been fed with standard diet (SD) or high-fat diet (HFD). The imaging-based 4-class tumor staging was used to follow pancreatic cancer development. Not fasting glycemia, 4-h fasting glycemia, insulin, C-peptide, glucose tolerance after OGTT and abdominal fat volume were measured during tumorigenesis.

Results PDAC development did not lead to an overt diabetic phenotype or to any alterations in glucose tolerance in KPC fed with SD. Consumption of *HFD* induced higher body weight/abdominal fat volume and worsened glucose homeostasis both in control CRE mice and only in early tumorigenesis stages of the KPC mice, excluding that the cancer development itself acts as a trigger for the onset of dysmetabolic features.

Conclusion Our data demonstrate that carcinogenesis in KPC mice is not associated with paraneoplastic diabetes.

Keywords Pancreatic cancer · KPC · High-fat diet · Diabetes · Staging

List of abbreviations

PDAC	pancreatic ductal adenocarcinoma
LSL	*loxP-STOP-loxP*
KPC	*LSL-Kras*$^{G12D/+}$, *LSL-Trp53*$^{R172H/+}$ and *Pdx-1-Cre* mice
CRE	*Pdx-1-Cre* mice
SD	standard diet
HFD	high-fat diet
ADTM	abdominal adipose tissue measurement
DM	diabetes mellitus
VNN1	vanin 1
T2D	type 2 diabetes
PanIN	pancreatic intraepithelial neoplasia
MRI	magnetic resonance imaging
OGTT	oral glucose tolerance test
AUC	area under the curve
A.U.	arbitrary unit
HOMA-IR	homeostatic model assessment for insulin resistance
AFV	abdominal fat volume
SEM	standard error
MR	magnetic resonance
KC	*LSL-Kras*$^{G12D/+}$ and *Pdx-1-Cre* mice
SD-KPC	standard diet-fed KPC

Managed by Antonio Secchi.

Electronic supplementary material The online version of this article (https://doi.org/10.1007/s00592-019-01335-4) contains supplementary material, which is available to authorized users.

Valentina Pasquale and Erica Dugnani equally contributed to this manuscript.

✉ Lorenzo Piemonti
piemonti.lorenzo@hsr.it

[1] Diabetes Research Institute, IRCCS San Raffaele Scientific Institute, Via Olgettina 60, 20132 Milan, Italy

[2] Division of Genetics and Cell biology, Genomic Unit for the diagnosis of human pathologies, IRCCS SanRaffaele Scientific Institute, 20132 Milan, Italy

[3] Department of Radiology, Experimental Imaging Center, IRCCS San Raffaele Scientific Institute, 20132 Milan, Italy

[4] Vita-Salute San Raffaele University, Milan, Italy

HFD-KPC high-fat diet-fed KPC
mPanc02 murine Panc02 cells

Introduction

Pancreatic ductal adenocarcinoma (PDAC) accounts for 85% of all pancreatic cancers. PDAC is refractory to current treatments in a context of a delayed diagnosis [1, 2] and early local and distal relapses, which makes it one of the most deadly cancers in the world [3]. Previous studies have investigated associations between diabetes (DM) and several cancers [4, 5], specifically between DM and PDAC [6]. Indeed, about 40–70% of patients with PDAC experienced diabetes or hyperglycemia [7, 8], which frequently manifests 2–3 years or less before diagnosis [6, 9]. Among diabetic patients, subjects with a new diagnosis of diabetes retain the highest risk (eightfold) to develop PDAC within 2 years compared to general population, while long-standing diabetes presents only a doubling of the risk [10]. The temporal association together with high prevalence of diabetes in patients suffering from PDAC [7] suggests two hypotheses: PDAC causes diabetes or diabetes shares risk factors for the development of PDAC. The hypothesis that diabetes may be tumor-induced, representing a paraneoplastic phenomenon, was supported by the identification of putative diabetogenic tumor-secreted molecules [9]. Among others, adrenomedullin was suggested to contribute to insulin secretion defect in vitro and in vivo tumor models [11], while islet amyloid polypeptide, S-100A8 N-terminal peptide and vanin 1 (VNN1) have been investigated as potential mediators of insulin resistance [12–14]. However, there are no compelling data in humans confirming their role. In contrast to the paraneoplastic diabetes hypothesis, we recently suggested that prevalence of DM in PDAC suffering patients is the same as chronic pancreatitis [6], a not neoplastic condition, and diabetes associated to PDAC is a clinical entity overlapping classical type 2 diabetes (T2D), for both risk factors and biochemical profile [7]. A demonstration other than epidemiological or observational evidences is needed to understand whether the aforementioned relationship has a causal link or it is a mere association. To properly address this issue, we studied the glucose homeostasis alteration associated with pancreatic cancer development in *LSL-Kras*$^{G12D/+}$*; LSL-Trp53*$^{R172H/+}$; and *Pdx-1-Cre* (KPC) mouse model [15]. KPC mice recapitulate the development of cognate human PDAC and spontaneously develop PDAC with 100% penetrance but in asynchronous manner, and consequently, the onset of pre-neoplastic lesions and PDAC is not age-related. For this reason, we applied an in vivo age-independent tumor staging system using high-resolution 7-Tesla magnetic resonance [16]. As a result, regardless of their age, KPC mice can be synchronized based on a specific phase of tumorigenesis. Moreover, we evaluated the glucose metabolism in mice fed with standard diet or a diet with 60% of energy derived from fat, mimicking an environmental risk factor shared between T2D and PDAC [17].

Materials and methods

Experimental design

The *LSL-Kras*$^{G12D/+}$*; LSL-Trp53*$^{R172H/+}$; and *Pdx-1-Cre* mice termed KPC (background C57BL/6 J) carrying mutated *Kras*^{G12D} and *Trp53*^{R172H} under the endogenous pancreatic promoter *Pdx-1* were obtained by Biogem (Avellino, Italy). Age-matched male and female *Pdx-1-Cre* (CRE) mice were used as controls. All mice were housed in the facility of preclinical imaging of San Raffaele Scientific Institute. At 2, 4 and 6 months of age, KPC and CRE mice were evaluated for (1) tumor staging; (2) glucose homeostasis and tolerance; and (3) abdominal fat volume (see Supplementary Fig. S1). Mice were euthanized by cervical dislocation when severe clinical symptoms or signs of advanced disease were displayed. At 6 weeks of age, KPC and CRE were allocated to either a purified high-fat diet (HFD) (Mucedola s.r.l., Italy) or a purified standard diet (SD) (Envigo, Italy) lifelong ad libitum. The analytical constituent rates in HFD and SD are, respectively, crude protein 23% and 18.6%, crude fibers 5% and 3.5%, crude ash 5.5% and 5.3% and crude fat 34% and 6.2%. HFD had the 60% of energy derived from fat in comparison with 18% of SD. Diets were replaced twice a week to avoid deterioration of HFD and changing of nutrient content.

Tumor staging and abdominal adipose tissue measurement (ADTM) using magnetic resonance imaging (MRI)

MRI was carried out to determine in vivo four-class tumor staging as previously described [16] using 7-Tesla MRI. The staging system ranked from stage 1 to stage 4; stage 1 and stage 2 identified mice with premalignant pancreatic alterations, while stage 3 and stage 4 detected an overt PDAC, respectively, <5 mm and ≥ 5 mm in diameter. For ADTM, T1-weighted sequences with and without fat saturation were acquired covering a body region from the hepatic dome to the inguinal canal (female)/scrotum (male). By means of image subtraction (T1–T1 fat), a "pure fat" result stack was obtained, on which a mask definition of adipose tissue along the abdominal fascia was manually drawn to segment all the intraperitoneal and retroperitoneal fat. After abdominal adipose tissue segmentation, volume quantification was semi-automatically performed using a region growing function. Abdominal fat volume (AFV) measurement was

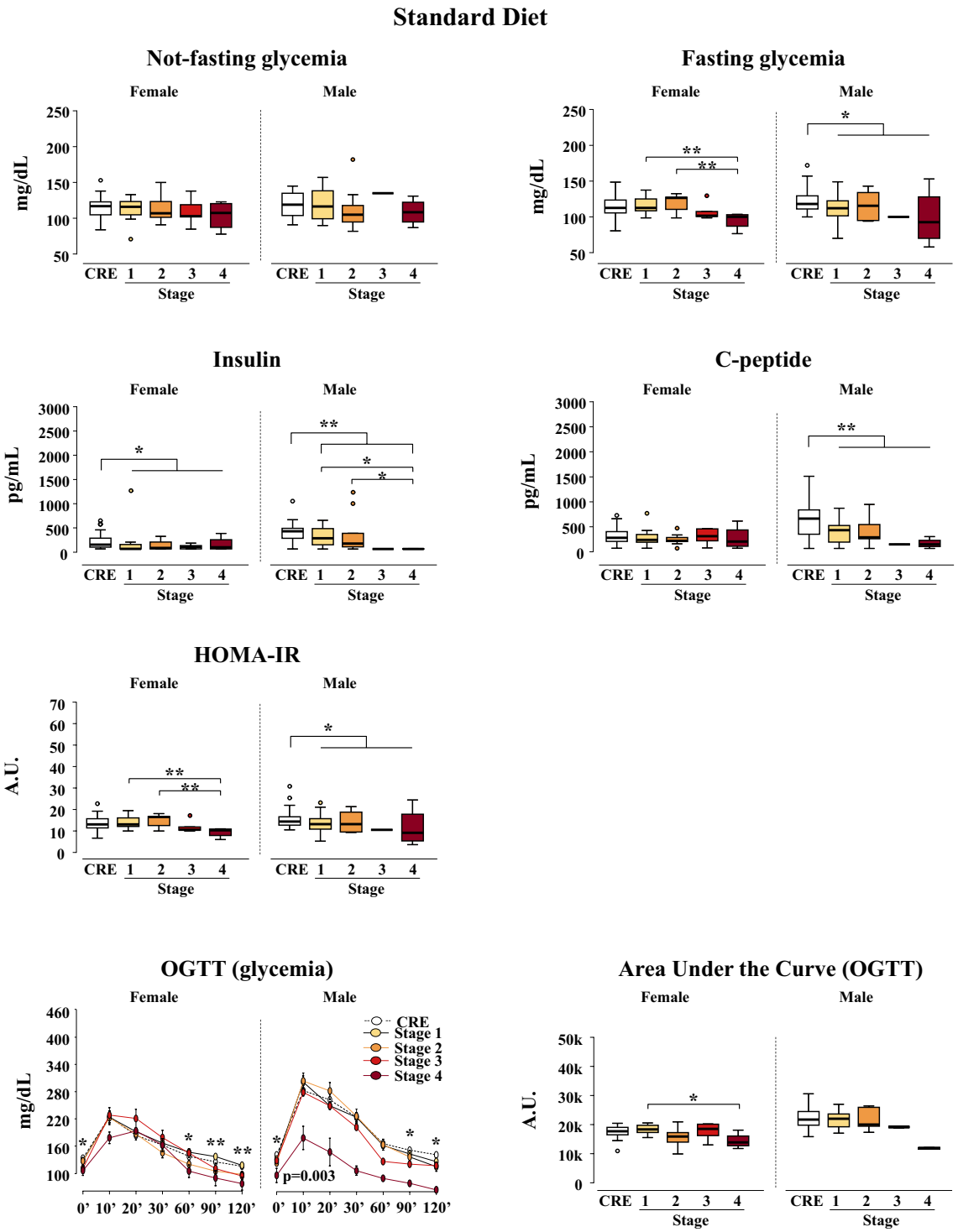

Fig. 1 Homeostasis of glucose in KPC mouse model fed with standard diet KPC ($n=26$; 14/12, female/male) and CRE mice ($n=27$; 16/11, female/male) were fed with standard diet and evaluated at 2, 4 and 6 months. Not fasting glycaemia, fasting glycaemia, fasting serum insulin, fasting serum C-peptide, HOMA-IR, glycemic profile and glucose area under the curve (AUC) during OGTT are represented according to the tumor stages. All data are represented as boxplots (white for CRE, yellow to dark red for stage 1 to stage 4 KPC) except for OGTT profile represented as mean ± SEM for each time points. Statistical analysis was performed by Mann–Whitney U test. For OGTT curves, statistical analysis was performed using general linear model among all groups and using Student's t-test within all groups in each time point. Only statistical significant differences are indicated between all CRE and all stage KPC or within KPC among stages: $*p<0.05$; $**p<0.01$; $***p<0.001$

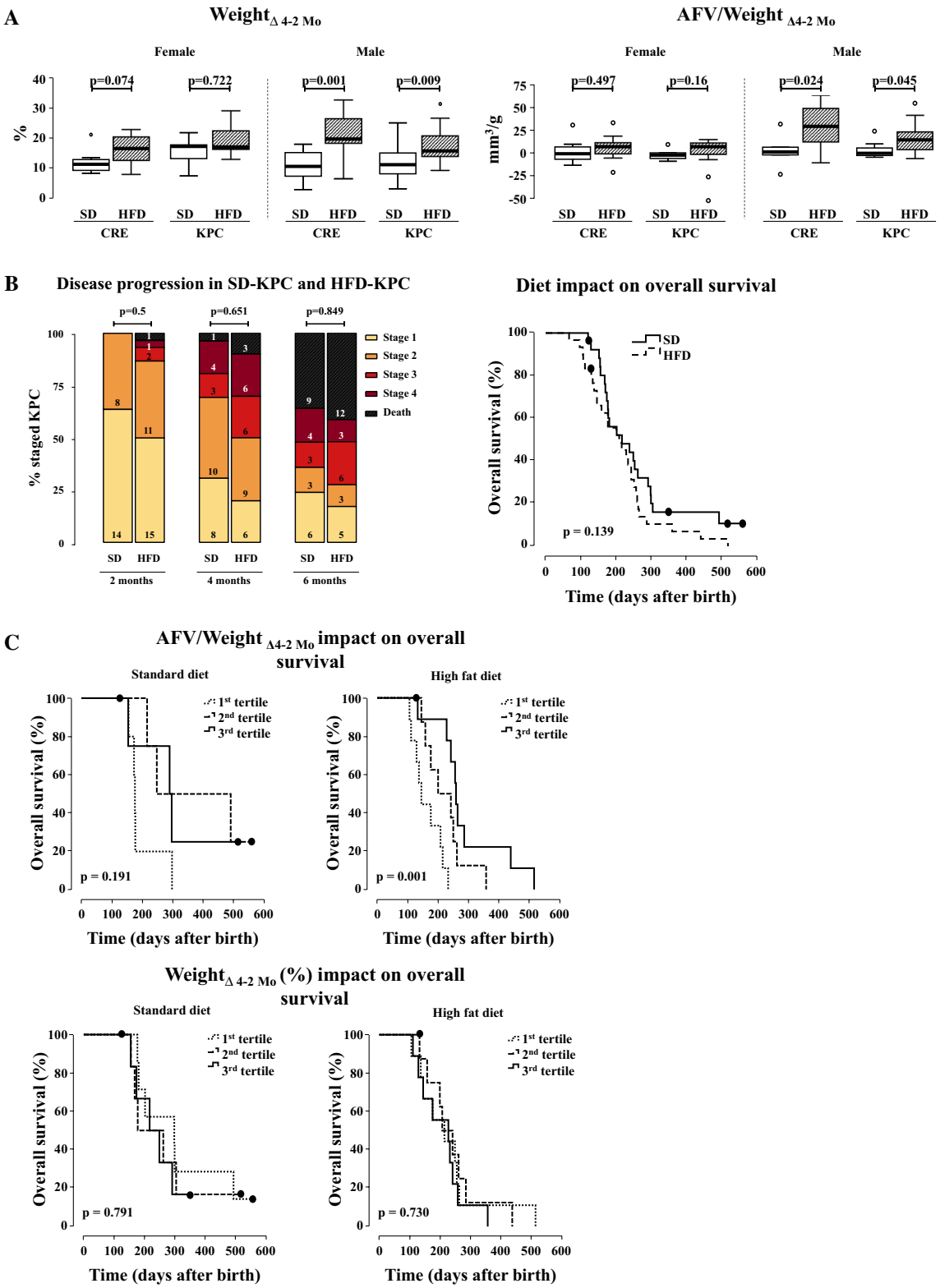

then normalized on mice weight obtaining the parameter AFV/weight (mm^3/g). Image processing and all the analyses were performed by a radiologist with 5-year experience in preclinical imaging of small rodents, using MIPAV [18] open-source software v.5.3.4 (and later versions). For further details, see supplementary methods.

◂**Fig. 2 Impact of diets on weight, abdominal fat volume, pancreatic cancer progression and survival in KPC mouse model** At 6 weeks of age, mice were allocated to a purified high-fat diet (HFD; KPC $n=30$, 14/16 female/male; CRE $n=28$, 13/15 female/male) lifelong ad libitum. Mice were evaluated at 2, 4 and 6 months of age and compared with mice fed with standard diet (SD). Panel A: the gain of body weight expressed as percentage ($weight_{\Delta\ 4-2\ Mo}$) and of weight-normalized abdominal fat volume expressed as mm^3/g (AFV/Weight $_{\Delta 4-2\ Mo}$) calculated from month 2 to month 4 of age; *p*-values were estimated by Mann–Whitney U test. Panel B: stage distribution between SD-fed KPC (SD-KPC) and HFD-fed KPC (HFD-KPC) at 2, 4 and 6 months of age; *p*-values were estimated by Pearson's chi-square test. The numbers into columns indicate the absolute number of mice. For each time point, cancer-related mortality was represented as a black bar. Four SD-KPCs at 2 months were not evaluated for technical problems. One HFD-KPC and one SD-KPC were not evaluated at 6 months because they died for cancer-unrelated reason. On the left, Kaplan–Meier survival curve for mortality from cancer according to diet; *p*-value was estimated by log-rank test. Panels C: Kaplan–Meier survival curve for mortality from cancer according to weight-normalized AFV (AFV/Weight $_{\Delta 4-2\ Mo}$) or weight increments (weight $_{\Delta 4-2\ Mo}$). Mice were categorized in tertiles (first from third tertile, lower to higher value, respectively). *P*-value was estimated by log-rank test

Glucose homeostasis and tolerance

Not fasting glycemia (Glucometer Elite, Bayer) and weight were measured twice a week for all survival time. Euglycemia was defined as not fasting blood glucose ≤ 200 mg/dL. Oral glucose tolerance test (OGTT) was performed at 2, 4 and 6 months of age: 1 g/kg of glucose was administrated by oral gavage after 4-hour fast. Blood glucose was determined at 0, 10, 20 30, 60, 90 and 120 min after glucose administration. The area under the curve (AUC) for glucose during OGTT was calculated using the trapezoidal method (baseline = 0 min). C-peptide and insulin were measured on serum after 4 h of fasting using multiplex assays based on Multi-Analyte Profile technology (MILLIPLEX MAP Mouse Metabolic Hormone Magnetic Bead panel). Assay was performed following the manufacturer's protocols and run on MAGPIX (Biorad) with Bio-Plex manager software v6.1 (Bio-Rad). Insulin resistance index (HOMA-IR) was calculated using the equation previously described [19]: arbitrary unit (A.U.) = [fasting blood glucose (mmol L^{-1}) * fasting insulin (mU L^{-1})]/14.1.

Statistical analysis

Data are summarized as mean ± standard error (SEM) and median with minimum–maximum or 25th–75th percentiles, according to their distribution. Variables with a normal distribution were compared with one-way unpaired Student's t-test or general linear model. Variables were compared using the Mann–Whitney U test or Pearson's chi-square test, as appropriated. Survival was evaluated using Kaplan–Meier analysis, and the significance was estimated using the log-rank test. *P*-value ≤ 0.05 was considered significant. All statistical analyses were performed using SPSS statistical software version 13.0 (SPSS Inc.) and GraphPad version 7 (GraphPad Software, Inc.).

Results

Pancreatic cancer development does not induced diabetes in KPC mice

In a first set of experiments, we tested the glucose homeostasis during pancreatic cancer development in KPC mice ($n=26$; 14/12, female/male) fed with standard diet (SD). As control group, CRE mice ($n=27$; 16/11, female/male) were analyzed. Fasting and not fasting blood glucose, fasting serum insulin, fasting serum C-peptide, insulin resistance (as HOMA-IR) and glucose tolerance (as OGTT) were evaluated as a function of tumor staging (Fig. 1) or age (Supplementary Fig. S2). All KPC and CRE mice showed a not fasting blood glucose level ≤ 200 mg/dL long-life (Fig. 1 and Supplementary Fig. S2A). Alterations mirroring (pre)diabetes were not observed regardless tumor staging. At the contrary, we observed an improvement in glucose tolerance (fasting and not fasting lower blood glucose, insulin and C-peptide levels associated with a decrement of HOMA-IR along with the increasing of the tumor stage (Fig. 1). To exclude that the obtained data were related to the KPC mice model, we also analyzed the glucose tolerance in a second surgical synchronous murine model of pancreatic cancer. Syngeneic pancreatic cancer cell lines Panc02 ($n=6$) or vehicle ($n=6$) were orthotopically injected into the pancreas of eight-week-old male C57BL/6 mice. Glucose metabolism was tested at three time points: the day before surgery, 30 days after surgery (early phase pancreatic cancer) and 50 day after surgery (advanced pancreatic cancer). All Panc02-injected mice developed pancreatic cancer, but none presented an impaired glucose tolerance (Supplementary Fig. S3). As for KPC mice, a better glucose tolerance was present at the advanced stage of pancreatic cancer. All these data together suggest that pancreatic cancer development did not result either in glucose intolerance or in diabetes.

Effect of high-fat diet on weight, abdominal fat volume and tumor development in KPC mice

In a second set of experiments, KPC mice ($n=30$; 14/16 female/male) and CRE ($n=28$; 13/15 female/male) were fed long-life with high-fat diet (HFD) starting from 6 weeks of age. As expected, at 4 months of age the median body weight increased more in HFD than

in SD-fed mice, especially in male animals (Fig. 2a). Concordantly, MRI showed an increased abdominal fat volume associated with the HFD (AFV/weight$_{\Delta 4-2\ Mo}$) (Fig. 2a). To assess the impact of HFD on tumor progression, we evaluated the distribution of MR-based tumor stages [16] at 2, 4 and 6 months of age and the overall survival (OS). Although the effect was not significant, KPC mice fed with HFD showed higher tumor stages as compared with the SD mice (Fig. 2b). Concordantly, a trend toward a shorter survival was present: The median survival times of mice fed with HFD and SD were 208 ± 35 and 216 ± 47 days, respectively ($p = 0.139$) (Fig. 2b). No sex-related differences were observed (Supplementary Figure S4). Finally, we evaluated whether AFV (AFV/weight$_{\Delta 4-2\ Mo}$) or weight increments from 2 to 4 months of age (Weight$_{\Delta 4-2\ Mo}$) induced by the HFD were associated with the overall survival. KPCs were divided in tertiles according to their increment both of AFV/weight$_{\Delta 4-2\ Mo}$ and of weight$_{\Delta 4-2\ Mo}$ (Fig. 2c). Higher abdominal fat volume was associated with a better OS (173 ± 13, 242 ± 28 and 264 ± 18 for first, second and third tertiles, $p = 0.001$) while weight increment appeared irrelevant (Fig. 2c).

High-fat diet does not push toward overt diabetes in KPC mouse during PDAC progression

As expected, we observed a worse glucose tolerance both for CRE and KPC fed with HFD than SD (Table 1), nevertheless none experienced an increase of glycemia above 200 mg/dL and all reached euglycemia after OGTT (Table 1, Fig. 3). As previously showed for SD, in HFD-fed KPC mice blood glucose (both fasting and not fasting), C-peptide level and HOMA-IR index showed a decrement along with the increasing of the tumor stage (Fig. 3). As for SD mice, a better glucose tolerance during OGTT was present at the advanced stage of pancreatic cancer (Fig. 3). Similar results were obtained when glucose metabolism was evaluated as a function of age (Supplementary Figure S5).

Discussion

The association between pancreatic cancer and diabetes relies on strong epidemiologic evidences [6, 8, 20, 21]. However, it is complicated to understand the etiopathogenesis of this association [6, 8, 22], whether diabetes is directly induced by tumor itself as a paraneoplastic syndrome [11, 12] or it is a subclinical disease with shared risk factors, unmasked by occurring rearrangement of pancreatic tissue during tumor development [7]. At our knowledge, this is the first study systematically addressing the glucose metabolism associated to cancer progression in genetically engineered mouse model of pancreatic cancer [23]. To address whether diabetes in PDAC can be explained as a paraneoplastic syndrome, we performed a characterization of glucose metabolism associated with pancreatic cancer development in the *LSL-Kras*$^{G12D/+}$; *LSL-Trp53*$^{R172H/+}$; and *Pdx-1-Cre* [15], a widely used genetically engineered mouse model of PDAC [24]. We decided to use both male and female mice to better depict all the spectrum of putative metabolic responses to PDAC progression; in fact, a recent report demonstrates the contribution of sex hormones to variation in insulin resistance in a strain-specific manner [25]. KPC recapitulates all the steps of carcinogenesis, from pre-neoplastic lesion to established cancer, with 100% penetrance but with variable latency. To overcome this issue, we used our recently published imaging-based staging method to grade tumor progression, in order to focus on specific phases of disease [16]. KPC mice did not experience any metabolic alterations toward diabetic, hyperglycemic or hyperinsulinemic status in standard dietary regimen. The obtained data do not seem to be linked to the specific genetic manipulation of the model, since also the orthotopic surgical models did not develop diabetes along with tumor progression. In agreement with our results, Zechner et al. [26] reported stable not fasting glucose concentration within 3 weeks after injection of three different lines in a syngeneic orthotopic pancreatic carcinoma model. Moreover, Danai et al. [23], studying the exocrine function and adipose wasting in pancreatic cancer, recently reported no insulin secretion defect in a different autochthonous mouse model of PDAC with Kras (G12D) activation and loss of Trp53 function via Trp53 deletion. Other studies, which sustained the paraneoplastic hypothesis and used in vivo models, are not in agreement with our results. Aggarwal et al. [11] observed only a slight changing in metabolic response to oral glucose tolerance test in athymic mice with subcutaneous or orthotopic injection of human pancreatic cancer cell line MPanc96 secreting adrenomedullin. Of note, we should underline the presence of some pitfalls like the use of only one pancreatic cell line, the choice of control group of mice subcutaneously and orthotopically injected with MPanc96 (wild-type instead of vehicle-injected mice) and the absence of glycaemia measurement during follow-up. Kang et al. [14] suggested that the daily intraperitoneal injection of supernatant from pancreatic cancer cell line transfected with putative diabetogenic factor VNN1 induces glucose intolerance in SCID mice. Again, there was only slight change within the euglycemic range for treated mice and, in addition, these anomalies did not persist for all the 30 days of treatment. These models, mainly aimed to explore the putative diabetogenic effect of cancer-secreted molecules, are also far from resembling the human disease. Indeed, this was our primary purpose with the KPC model, a model reproducing faithfully all the steps of human disease, including pre-neoplastic lesions (relevant in the study of

Table 1 Parameters involved in glucose homeostasis: comparison between high-fat diet and standard diet

Female				Male		
	SD	HFD	*p*	SD	HFD	*p*
	Median [25th–75th]	Median [25th–75th]		Median [25th–75th]	Median [25th–75th]	
Not fasting glycemia (mg/dL)						
CRE	117 [105–123]	126 [117–133]	***0.004***	119 [103–136]	146 [136–156]	***<0.001***
Stage 1	116 [104–125]	127 [111–139]	*0.066*	117 [98–139]	129 [118–149]	0.268
Stage 2	107 [99–126]	145 [110–154]	***0.033***	105 [94–122]	120 [112–159]	*0.079*
Stage 3	103 [94–129]	110 [101–125]	0.754	135[a]	113 [108–140]	0.600
Stage 4	108 [83–122]	105 [103–109]	0.915	109 [91–127]	108 [90–144]	0.773
Fasting glycemia (mg/dL)						
CRE	117 [105–123]	126 [117–133]	***0.001***	118 [110–133]	155 [140–174]	***<0.001***
Stage 1	112 [107–128]	124 [113–147]	*0.087*	112 [101–126]	135 [120–157]	***0.002***
Stage 2	126 [109–127]	137 [122–147]	*0.057*	116 [95–135]	137 [125–157]	***0.019***
Stage 3	101 [99–118]	112 [103–125]	0.402	100[a]	129 [114–143]	0.117
Stage 4	100 [81–103]	102 [86–106]	0.666	93 [64–141]	109 [76–131]	0.773
Insulin (pg/mL)						
CRE	154 [103–294]	86 [69–204]	***0.031***	433 [286–500]	522 [358–903]	***0.011***
Stage 1	69 [69–195]	91 [69–152]	0.972	289 [157–503]	177 [69–292]	*0.07*
Stage 2	87 [69–259]	92 [72–388]	0.332	180 [91–699]	273 [115–354]	0.950
Stage 3	107 [69–161]	69 [69–247]	0.410	69[a]	267 [134–324]	0.162
Stage 4	100 [69–322]	96 [69–186]	1.000	69 [69–75]	316 [74–826]	0.091
C–peptide (pg/mL)						
CRE	276 [200–403]	499 [326–615]	***0.001***	664 [349–841]	1169 [552–1756]	***0.001***
Stage 1	236 [175–371]	405 [358–601]	*0.057*	434 [174–533]	654 [274–985]	*0.085*
Stage 2	215 [201–310]	412 [326–507]	***0.018***	290 [184–616]	881 [666–1073]	***0.007***
Stage 3	309 [146–457]	363 [258–747]	0.347	150[a]	1161 [561–1592]	0.117
Stage 4	202 [88–522]	467 [194–715]	0.336	152 [88–268]	518 [388–1183]	***0.021***
HOMA–IR (A.U.)						
CRE	13 [11.4–15.8]	16.7 [13.5–20.9]	***0.001***	14.2 [12.6–18.3]	24.7 [20.2–31.3]	***<0.001***
Stage 1	13 [11.9–17]	15.9 [13.2–22.4]	*0.087*	13 [10.5–16.4]	18.9 [14.9–25.6]	***0.002***
Stage 2	16.5 [12.3–16.7]	19.5 [15.3–22.3]	*0.057*	13 [9.4–19.3]	19.3 [16.1–25.6]	***0.027***
Stage 3	10.6 [10.2–14.6]	13 [11–16.2]	0.402	10.4[a]	17.3 [13.4–21.2]	0.117
Stage 4	10.3 [6.9–10.9]	10.8 [7.8–11.7]	0.666	9 [4.4–21]	12.5 [6.1–17.7]	0.773
AUC OGTT (AU)						
CRE	17,733 [16,401–19,103]	20,893 [18,759–23,409]	***<0.001***	21,735 [19,650–24,760]	26,990 [24,495–30,496]	***<0.001***
Stage 1	18,355 [17,065–19,795]	21,330 [19,955–24,985]	***0.002***	22,013 [19,169–24,166]	29,170 [25,865–31,685]	***<0.001***
Stage 2	15,945 [12,980–17,610]	20,355 [19,700–25,480]	***0.004***	20,030 [19,138–25,965]	28,080 [25,868–31,003]	***0.002***
Stage 3	18,545 [14,683–20,215]	20,470 [18,375–24,790]	0.117	19,175[a]	31,135 [28,651–36,588]	0.121
Stage 4	13,923 [12,331–17,123]	19,090 [13,250–19,103]	0.219	11,920[b]	15,948 [7626–30,921]	0.355

[a]single value; [b]mean value of 2 mice. Statistical analyses were estimated by Mann–Whitney U test

SD standard diet; *HFD* high-fat diet; *AU* arbitrary units

p-value ≤ 0.05 is in bold and italics; *p*-value ≤ 0.1 is in italics

glucose metabolism modification, which arises in the early phase of the tumor progression).

As KPC model did not experience metabolic changes toward diabetes, we hypothesized that the pancreatic cancer alone was not enough to induce diabetes and we exposed KPC to a well-recognized environmental risk factor for both diabetes and PDAC [17], a diet with high-fat content. HFD induced the same impairment of glucose homeostasis both in control CRE mice and only in premalignant phases (stages 1–2) of the KPC mice, excluding that the cancer development itself acts as a trigger for the onset of dysmetabolic features. Of note, previous studies made on models of PDAC [27–30] reported a significant impact of HFD on overall survival and disease progression. A similar trend was

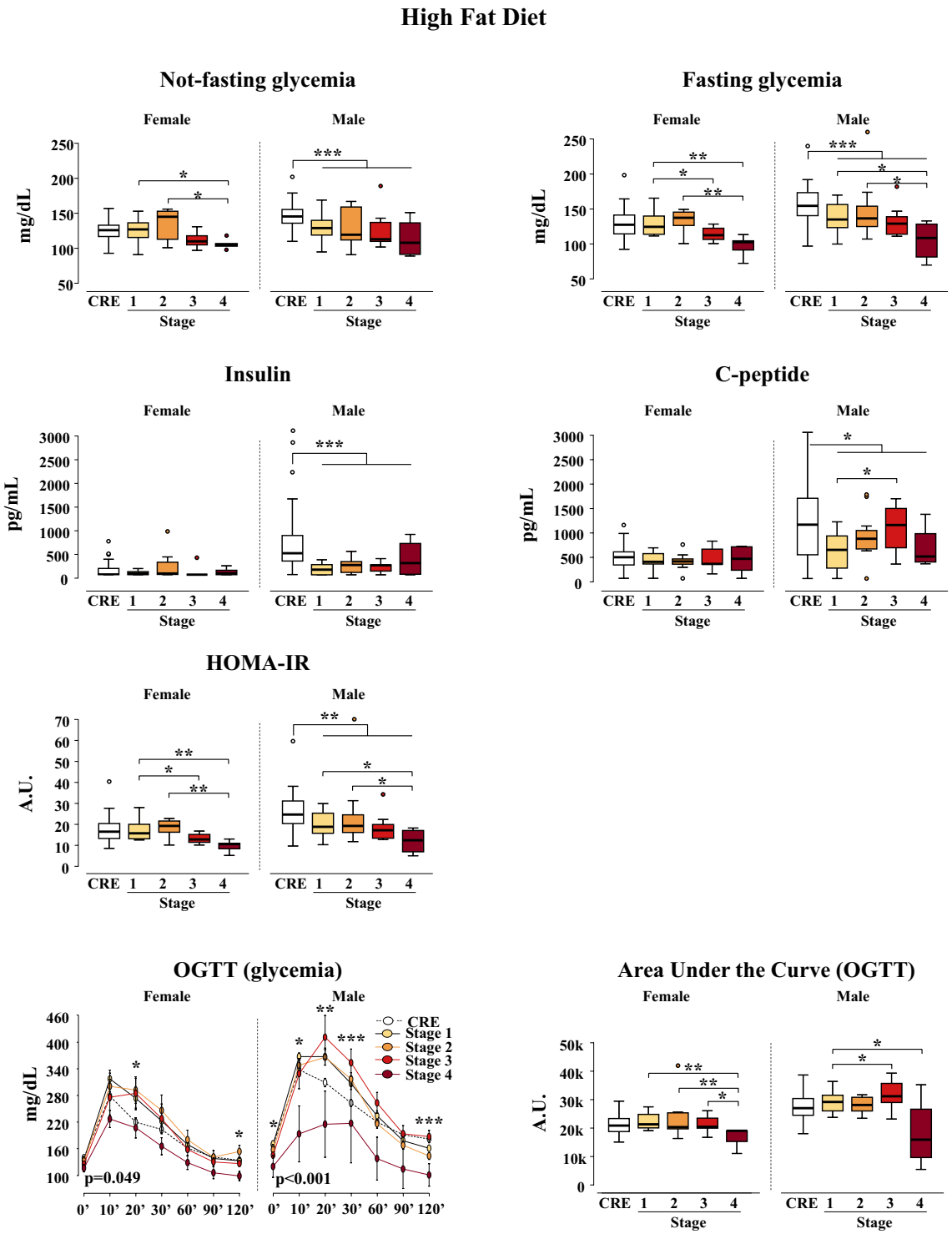

Fig. 3 Homeostasis of glucose in KPC mouse model fed with high-fat diet KPC ($n=30$; 14/16 female/male) and CRE mice ($n=28$; 13/15, female/male) were fed with high-fat diet (HFD) and evaluated at 2, 4 and 6 months. Not fasting glycaemia, fasting glycaemia, fasting serum insulin, fasting serum C-peptide, HOMA-IR, glycemic profile and glucose area under the curve (AUC) during OGTT are represented according to the tumor stages. All data are represented as boxplots (white for CRE, yellow to dark red for stage 1 to stage 4 KPC) except for OGTT profile represented as mean ± SEM for each time points. Statistical analysis was performed by Mann–Whitney U test. For OGTT curves, statistical analysis was performed using general linear model among all groups and using Student's t-test within all groups in each time point. Only statistical significant differences are indicated between all CRE and all stage KPC or within KPC among stages: *$p<0.05$; **$p<0.01$; ***$p<0.001$

also present in our KPC mice fed with HFD, but quantitatively this was less relevant than in previous reports [27–30]. This relative discrepancy can be explained by the different model and by the different methodologies used to analyze the disease progression. Previous works were mainly based on the observation of precursor lesion occurrence in *LSL-Kras*$^{G12D/+}$ and *Pdx-1-Cre* (KC) murine model, harboring a single mutation in *Kras* which results in an incomplete penetrance of PDAC and a slow progression of the disease. Moreover, the disease progression was quantified by the frequencies of neoplastic lesions detected postmortem in histological analyses. This prevented a complete follow-up and the possibility to observe a "clinical" change in PDAC progression [27–29]. Unlike those studies, we synchronized KPC mice on a specific stage (from stage 1 to stage 4) based on our published four-class tumor staging system using 7 T magnetic resonance and we were able to follow disease development and progression through time on the same mouse [16]. The evidence of a better glucose tolerance and an increased insulin sensitivity at the advanced stage of pancreatic cancer compared with early stages deserves a discussion. We can speculate on a lower basal secretion of insulin due to a lower sugar level in the blood as a consequence of the high glycolytic phenotype of the tumor [31, 32]. In fact, the tumor burden associated with stage 4 disease could induce insulin-independent glucose consumption. Accordingly, aberrant pancreatic GLUT1 expression was detected in PDAC [33, 34].

We also evaluated whether weight and abdominal fat increment could influence survival. A higher AFV was associated with a better overall survival. We can speculate that adipose tissue deposits may represent an index of a better nutritional status. Nutritional status in pancreatic cancer patients is crucial to obtain a better outcome, as demonstrated by studies on the prognostic nutritional index [35, 36]. For mice, abdominal adipose tissue could represent a useful reservoir to counteract the huge energy expenditure linked to cancer development.

One of the major limits of mouse model to study the association between pancreatic cancer and diabetes is the relative inadequacy of the model to reproduce the role of chronic reactive pancreatitis. If we set apart the hypothesis of paraneoplastic diabetes, the role of the reactive pancreatitis, frequently present also in the early stage of pancreatic cancer, cannot be ruled out in the ontogeny of diabetes associated to PDAC in humans [37, 38]. We demonstrated that patients suffering from chronic pancreatitis have high prevalence of diabetes as well as PDAC patients [6]. In mouse, it described the impossibility to induce obstructive pancreatitis despite the use of invasive surgery, such as closed duodenal loop or simultaneous bile and pancreatic duct obstruction [39]. Therefore, there is the possibility that pancreatic cancer alone is not able to induce pancreatitis in mouse as that observed in humans. To bypass this problem, the model could be improved in the future by introducing caerulin treatment, a cholecystokinin analogue that administered *intra-peritoneum* induces abnormal release of active enzyme directly in the pancreas [39], mimicking the pancreatitis process.

In conclusion, taken together, our results claim that the role of tumor-released factor/s in the etiopathogenesis of cancer-associated diabetes is doubtful.

Acknowledgements This study was supported by the Associazione Italiana per la Ricerca sul Cancro (AIRC, bando 5 X 1,000 N_12182).

Authors' contributions VP, ED and LP contributed to study concept and design; VP, ED, DL, PM, AC, TC, MP and LV helped in acquisition of data; VP, ED, PM, AE and LP contributed to analysis and interpretation of data; VP, ED and LP contributed to statistical analysis of data; VP, ED, DL and LP helped in drafting of the manuscript; and AE, LP contributed to critical revision of the manuscript. All authors have approved the submitted manuscript.

Compliance with ethical statement

Conflict of interest The authors have nothing to disclose.

Ethics statement This study was approved by the Animal Care and Use Committee of San Raffaele Scientific Institute (IACUC number 559) and performed in accordance with their guidelines.

Informed consent For this type of study informed consent is not required.

References

1. Hidalgo M (2010) Pancreatic cancer. N Engl J Med 362(17):1605–1617
2. Zhou B et al (2017) Early detection of pancreatic cancer: where are we now and where are we going? Int J Cancer 141(2):231–241. https://doi.org/10.1002/ijc.30670
3. Lucas AL et al (2016) Global trends in pancreatic cancer mortality from 1980 through 2013 and predictions for 2017. Clin Gastroenterol Hepatol 14(10):1452–1462 e4
4. Wei M et al (2017) The need for differentiating diabetes-specific mortality from total mortality when comparing metformin with insulin regarding cancer survival. Acta Diabetol 54(2):219–220
5. Yang WS et al (2017) Association between type 2 diabetes and cancer incidence in Taiwan: data from a prospective community-based cohort study. Acta Diabetol 54(5):455–461
6. Balzano G et al (2014) Clinical signature and pathogenetic factors of diabetes associated with pancreas disease (T3cDM): a prospective observational study in surgical patients. Acta Diabetol 51(5):801–811
7. Dugnani E et al (2016) Diabetes associated with pancreatic ductal adenocarcinoma is just diabetes: results of a prospective observational study in surgical patients. Pancreatology 16(5):844–852

8. Pannala R et al (2008) Prevalence and clinical profile of pancreatic cancer-associated diabetes mellitus. Gastroenterology 134(4):981–987
9. Sah RP et al (2013) New insights into pancreatic cancer-induced paraneoplastic diabetes. Nat Rev Gastroenterol Hepatol 10(7):423–433
10. Chari ST et al (2005) Probability of pancreatic cancer following diabetes: a population-based study. Gastroenterology 129(2):504–511
11. Aggarwal G et al (2012) Adrenomedullin is up-regulated in patients with pancreatic cancer and causes insulin resistance in beta cells and mice. Gastroenterology. 143(6):1510–1517 e1
12. Basso D et al (2006) Pancreatic cancer-derived S-100A8 N-terminal peptide: a diabetes cause? Clin Chim Acta 372(1–2):120–128
13. Basso D et al (2011) Altered intracellular calcium fluxes in pancreatic cancer induced diabetes mellitus: relevance of the S100A8 N-terminal peptide (NT-S100A8). J Cell Physiol 226(2):456–468
14. Kang M et al (2016) VNN1, a potential biomarker for pancreatic cancer-associated new-onset diabetes, aggravates paraneoplastic islet dysfunction by increasing oxidative stress. Cancer Lett 373(2):241–250
15. Hingorani SR et al (2005) Trp53R172H and KrasG12D cooperate to promote chromosomal instability and widely metastatic pancreatic ductal adenocarcinoma in mice. Cancer Cell 7(5):469–483
16. Dugnani E et al (2018) Four-class tumor staging for early diagnosis and monitoring of murine pancreatic cancer using magnetic resonance and ultrasound. Carcinogenesis 39(9):1197–1206
17. Garg SK et al (2014) Diabetes and cancer: two diseases with obesity as a common risk factor. Diabetes Obes Metab 16(2):97–110
18. McAuliffe MJ et al (2001) Medical image processing, analysis and visualization in clinical research. In: Proceedings 14th IEEE symposium on computer-based medical systems. CBMS 2001
19. van Dijk TH et al (2013) A novel approach to monitor glucose metabolism using stable isotopically labelled glucose in longitudinal studies in mice. Lab Anim 47(2):79–88
20. Ben Q et al (2011) The relationship between new-onset diabetes mellitus and pancreatic cancer risk: a case-control study. Eur J Cancer 47(2):248–254
21. Li D et al (2011) Diabetes and risk of pancreatic cancer: a pooled analysis of three large case-control studies. Cancer Causes Control 22(2):189–197
22. Chari ST et al (2008) Pancreatic cancer-associated diabetes mellitus: prevalence and temporal association with diagnosis of cancer. Gastroenterology 134(1):95–101
23. Danai LV et al (2018) Altered exocrine function can drive adipose wasting in early pancreatic cancer. Nature 558(7711):600–604
24. Lee JW et al (2016) Genetically engineered mouse models of pancreatic cancer: the KPC model (LSL-Kras(G12D/+);LSL-Trp53(R172H/+);Pdx-1-Cre), its variants, and their application in immuno-oncology drug discovery. Curr Protoc Pharmacol 73:14 39 1–14 39 20
25. Parks BW et al (2015) Genetic architecture of insulin resistance in the mouse. Cell Metab 21(2):334–346
26. Zechner D et al (2015) Characterization of novel carcinoma cell lines for the analysis of therapeutical strategies fighting pancreatic cancer. Cell Biosci 5:51
27. Khasawneh J et al (2009) Inflammation and mitochondrial fatty acid beta-oxidation link obesity to early tumor promotion. Proc Natl Acad Sci U S A 106(9):3354–3359
28. Cheon EC et al (2011) Alteration of strain background and a high omega-6 fat diet induces earlier onset of pancreatic neoplasia in EL-Kras transgenic mice. Int J Cancer 128(12):2783–2792
29. Dawson DW et al (2013) High-fat, high-calorie diet promotes early pancreatic neoplasia in the conditional KrasG12D mouse model. Cancer Prev Res (Phila) 6(10):1064–1073
30. Philip B et al (2013) A high-fat diet activates oncogenic Kras and COX2 to induce development of pancreatic ductal adenocarcinoma in mice. Gastroenterology 145(6):1449–1458
31. McDevitt TM, Tisdale MJ (1992) Tumour-associated hypoglycaemia in a murine cachexia model. Br J Cancer 66(5):815–820
32. Liang C et al (2016) Energy sources identify metabolic phenotypes in pancreatic cancer. Acta Biochim Biophys Sin (Shanghai) 48(11):969–979
33. Basturk O et al (2011) GLUT-1 expression in pancreatic neoplasia: implications in pathogenesis, diagnosis, and prognosis. Pancreas 40(2):187–192
34. Yu M et al (2015) Metabolic phenotypes in pancreatic cancer. PLoS ONE 10(2):e0115153
35. Geng Y et al (2015) Prognostic nutritional index predicts survival and correlates with systemic inflammatory response in advanced pancreatic cancer. Eur J Surg Oncol 41(11):1508–1514
36. Balzano G et al (2017) A preoperative score to predict early death after pancreatic cancer resection. Digest Liver Dis 49(9):1050–1056
37. Kimura Y, Kikuyama M, Kodama Y (2015) Acute pancreatitis as a possible indicator of pancreatic cancer: the importance of mass detection. Intern Med 54(17):2109–2114
38. Bracci PM et al (2009) Pancreatitis and pancreatic cancer in two large pooled case-control studies. Cancer Causes Control 20(9):1723–1731
39. Chan YC, Leung PS (2007) Acute pancreatitis: animal models and recent advances in basic research. Pancreas 34(1):1–14